DEVELOPMENTAL BIOLOGY **173,** 265–278 (1996)
Article No. 0022

Formation and Maturation of the Calcium Release Apparatus in Developing and Adult Avian Myocardium

Feliciano Protasi, Xin-Hui Sun, and Clara Franzini-Armstrong

Department of Cell and Developmental Biology, University of Pennsylvania, School of Medicine, Philadelphia, Pennsylvania 19104–6058

Muscle fibers release large amounts of calcium from an internal compartment, the sarcoplasmic reticulum (SR), during activation. Two proteins are involved in this process and its control: plasma membrane calcium channels, or dihydropyridine receptors (DHPRs), and SR calcium release channels, or ryanodine receptors (RyRs). The two proteins form part of a structural complex, perhaps unique to muscle cells, which allows an interaction between plasma membrane and SR, resulting in calcium release from the latter. The surface–SR interaction is a step in the coupling between electrical events in the plasma membrane and contraction (excitation–contraction coupling). The structural complexes have been called calcium release units. One key to further understanding the control of calcium homeostasis in muscle is knowledge of how DHPRs and RyRs assemble into calcium release units. We have studied the development of avian myocardium, using immunocytochemistry to locate DHPRs and RyRs and electron microscopy to follow the formation of calcium release units containing feet (RyRs) and large membrane particles (presumably DHPRs). We find that the initial step is a docking of SR vesicles to the plasma membrane, followed by the appearance of feet in the junctional gap between SR and plasma membrane. Feet aggregate in ordered arrays, and the arrays increase in size until they fill the entire junctional gap. Clustering of membrane particles, presumably DHPRs, is apparently coupled to clustering of feet, since the two junction components assemble within patches of membrane of approximately equal size and containing an approximately constant ratio of particles to feet. Thus, despite the fact that no evidence exists for a direct interaction between DHPRs and RyRs in cardiac muscle, some mechanism exists to ensure that the two molecules are clustered in proximity to each other and in the appropriate proportion.

INTRODUCTION

All cells have internal calcium storage compartments which accumulate calcium by means of calcium pumps of the SERCA family (for reviews see MacLennan and Toyofuku, 1992; Pozzan *et al.,* 1994). Release of calcium from these compartments occurs through two related calcium release channels, the IP_3 receptors (Berridge and Irvine, 1989; Takei *et al.,* 1994) and the ryanodine receptors, or RyRs[1] (Inui *et al.,* 1987 a,b; Lai *et al.,* 1988; Anderson *et al.,* 1989; Giannini *et al.,* 1995). Muscle fibers have an extensive Ca^{2+} storage compartment, the sarcoplasmic reticulum (SR). The SR is rich in RyRs (see Meissner, 1994, for a review), localized mostly in specialized junctional domains (jSR; Franzini-Armstrong and Jorgensen, 1994).

Calcium release from the SR is part of a process termed excitation–contraction (e–c) coupling. This is initiated by depolarization of the plasma membrane and its invaginations, the transverse (T) tubules. Depolarization is sensed by calcium channels, the dihydropyridine receptors or DHPRs, located in the plasma membrane and T tubules (for reviews, see Ashley *et al.,* 1991; Catterall, 1991; Stern and Lakatta, 1992; see also Cannell *et al.,* 1995). DHPRs and RyRs are in close proximity at sites where junctional domains of the SR, bearing arrays of RyRs, are closely apposed to junctional domains of the plasma membrane (jPM) or transverse tubules (jT), containing DHPRs (Jorgensen *et al.,* 1989; Flucher *et al.,* 1990; Yuan *et al.,* 1991, Carl *et al.,* 1995; Sun *et al.,* 1995). This DHPRs–RyRs association has so far been detected only in muscle fibers, and the structures

[1] Abbreviations used: SR, sarcoplasmic reticulum; DHPR, dihydropyridine receptor or L-type calcium channel; RyR, ryanodine receptor or calcium release channel; SERCA, sarco/endoplasmic reticulum Ca^{2+}–ATPase; jSR, junctional domains of the sarcoplasmic reticulum; e–c coupling, excitation–contraction coupling; T tubules, transverse tubules; jT, junctional domains of the transverse tubules; jPM, junctional domains of the plasma membrane.

0012-1606/96 $12.00

in which this occurs are called either calcium release units or e–c coupling units, depending on the role they play. Calcium release units in muscle are uniquely designed for the rapid and controlled release of the large amount of calcium that is needed for activation of contraction. Our aim is to define how these unique assemblies are formed during development of cardiac muscle.

In this work, we take advantage of the fact that RyRs and DHPRs are visible in the electron microscope. The cytoplasmic domains of RyRs form the ''feet,'' linking jSR to jT or jPM (Block *et al.*, 1988). DHPRs have been identified with large intramembrane particles, seen in freeze-fracture replicas of jPM and jT in skeletal muscle (Block *et al.*, 1988; Franzini-Armstrong *et al.*, 1991; Takekura *et al.*, 1994a). A similar identification has been proposed for cardiac muscle (Sun *et al.*, 1995).

We address the following questions: (1) It is known that RyRs are detectable at very early stages in cardiac muscle (Dutro *et al.*, 1993). Is the formation of calcium release units also an early developmental event? (2) What are the sequential steps involved in the association of RyRs and DHPRs with the junctions? (3) Is there an obligatory relationship between DHPRs and RyRs during the formation of calcium release units? (4) What steps lead to the maturation of the membrane system from its initial formation to the adult arrangement?

Our results indicate the following sequential steps in the formation of the junction: an initial docking of the SR membrane to the plasmalemma, the formation of arrays of feet, and the parallel clustering of large particles (presumably DHPRs) in the jPM domains. Arrays of feet and clusters of large particles grow in parallel, until the junctional gap is completely filled by feet. An obligatory relationship between the locations and quantities of DHPRs and RyRs is apparently established early during development and maintained throughout. As in skeletal muscle, we can define a maturation phase, in which the e–c coupling system adapts itself to the higher demands of larger and more active cells. This involves an increase in size and frequency of junctions, the acquisition of a regular disposition of junctions relative to the sarcomere, and finally the development of the internal extended jSR.

MATERIALS AND METHODS

Chick embryos at 2.5 to 21 days of incubation (E2.5–E21), young chicks at 1 to 14 days after hatching (D1–D14), and adult chickens were used.

Immunohistochemistry

For immunofluorescent labeling, hearts (E10 to adult) were removed and perfused through the aorta with a ''relaxing'' solution (80 m*M* potassium acetate, 10 m*M* potassium phosphate buffer, 5 m*M* EGTA). After ~5 min, portions of the left ventricle were frozen in liquid nitrogen-cooled propane. Hearts at E2.5–E7 were bisected in the relaxing solution and then frozen. Cryostat sections (12–15 μm thick) were cut at −20°C.

Antibodies used were: (a) CR2, a rabbit polyclonal antibody raised against a fragment of rabbit cardiac α_1DHPR derived from a plasmid for the 549 C-terminus amino acids (Yoshida *et al.*, 1992). This antibody immunolabels chick cardiac muscle (Sun *et al.*, 1995). (b) 34C, a mouse monoclonal antibody, generously provided by Dr. J. Sutko and Dr. J. A. Airey, which recognizes α, β, and avian cardiac RyR (Airey *et al.*, 1990).

The unfixed sections were incubated for 1 hr each in 1% bovine serum albumin in PBS (PBS/BSA), followed by either CR2 or 34C and by Texas red-conjugated goat anti-mouse IgG (from Molecular Probes Inc.) and goat anti-rabbit IgG (from Cappel products), all diluted in PBS/BSA. In control experiments, cryosections were incubated in 1% PBS/BSA for 2 hr, followed by one of the secondary antibodies. The specimens were viewed in a scanning confocal microscope (Bio-Rad MRC-600, Microscience).

Electron Microscopy

Hearts at E10–adult were perfused either with a ''relaxing'' solution as above, or with a ''Ca^{2+} free solution'' (0.9% NaCl, 10 m*M* potassium–phosphate buffer, 10 m*M* EGTA, pH 7.4), which also maintains the myocardium in a relaxed state. Smaller hearts were immersed and bisected in either solution. Fixation with 3.5% glutaraldehyde in 0.1 *M* cacodylate buffer, pH 7.4, was also by either perfusion or immersion. Either the whole heart (at E2.5–E4) or small pieces of the left ventricle were postfixed in 2% OsO_4 in cacodylate buffer for 2 hr, block-stained in saturated uranyl acetate at 60°C for 4 hr, and embedded in Epon 812. Thin sections were stained in uranyl acetate and lead.

For freeze-fracture, bundles were similarly fixed in either 3.5 or 6% glutaraldehyde, infiltrated in 30% glycerol, frozen in liquid nitrogen-cooled propane, fractured, shadowed with platinum at 45°C, and replicated with carbon in a Balzer's 400. The replicas and thin sections were photographed in a Philips EM 410.

Measurements

Sizes of peripheral couplings and junctional plasma membrane domains (see Results) were measured from images collected by photographing the relevant structures as they first appeared on the EM screen until it was decided that a sufficiently large sample had been obtained. In the case of freeze-fractures at E4 and E6, this involved a prolonged search, because limited views of the surfaces are available and the particle domains are small and rare. It is possible that very small domains were missed in this search.

Areas of junctions were estimated by measuring the length of apposition between profiles of jSR and jPM in sections perpendicular to the two apposed membranes. Assuming that the junction is circular and that images of sections cutting across it (such as those in Figs. 6B, 6C, 6E, and 6G) represent random chords of such circles, the average

measured chord (y) is related to the diameter of the average circle (D) by the equation: $y = \pi D/4$.

The outline of plasma membrane domains was marked on images from freeze-fracture replicas, and their surface areas were directly measured. Large membrane particles within the domains were visually identified and counted. We have previously shown that visual identification selects a type of particle which is significantly different in height and size relative to the average extrajunctional particle (Sun *et al.*, 1995).

Images for measuring the size of the junctional gap were selected from the initial random collection using the following criteria: crispness of the membrane profile, indicating a good cross section of the membrane, and good focus (comparable to that shown in Figs. 6B, 6C, 6E, and 6G). Lines were drawn on the print at several random positions across the junctions, and measurements of the junctional gap were done with a dissecting microscope equipped with an eyepiece micrometer.

For counting the frequency of peripheral couplings, all plasma membrane profiles in a section were divided into 0.8-μm-long segments, the number of peripheral couplings in each segment were counted, and data from 10 adjacent segments were pooled. The number of profiles per 100-μm length of plasma membrane profile was calculated, assuming that the membrane is straight through the segment. The error resulting from this approximation is small, considering the short length of the segment, but it is slightly larger at younger ages, where the fixed membrane is wrinkled.

Although only one animal was used at each time point, all significance tests were performed using data from three to four animals from neighboring time points so that the sample size was statistically appropriate.

RESULTS

Clusters of RyRs and DHPRs

Avian cardiac muscle was selected because it lacks T tubules and thus complete calcium release units are located at the plasma membrane. Images in Fig. 1 illustrate cross sections of the left ventricle at E7 (Figs. 1A and 1B), E10 (Figs. 1C and 1D), D1 (Figs. 1E and 1F), and adult (Figs. 1G and 1H), immunolabeled for DHPR (left) and RyR (right). RyRs and DHPRs are located in small clusters along the cells' periphery. In the early developmental stages, particularly at E7 and E10, high gain and a wide open return aperture had to be used in order to detect foci of the two proteins in the confocal microscope. Detection became easier with increasing embryonic and postembryonic ages, indicating an increment in protein content of the clusters. As the cells enlarge, the number of spots per cell outline also increases. However, due to differences in signal gain and in the size of the return aperture used in collecting the data, a quantitative assessment of changes in frequency of spots between early and late stages is not possible from these images. In the adult, internal RyR-positive spots probably represent corbular SR, i.e., SR bearing a group of feet but not associated with the plasma membrane (Jewett *et al.*, 1971, 1973; Sommer and Johnson, 1979; Dolber and Sommer, 1984).

We were unable to detect foci of either protein in frozen sections at E6 or in whole mounts of hearts at E3 and E4. The latter were permeabilized by a 10-min exposure to MeOH at −20°C. We do not know if this failure is due to a technical limitation (the sections at E6 were very poor and infiltration of the whole heart may be limited) or to the small size of RyR and DHPR aggregates at these early ages (see below).

Colocalization of the two proteins in closely apposed hot foci was shown at D6 and D10 in a previously published work (Sun *et al.*, 1995).

Peripheral Couplings and Plasma Membrane Domains

Peripheral couplings and junctional plasma membrane domains (jPM) are defined in electron microscope images of thin sections and freeze-fracture replicas.

Well-developed peripheral couplings are junctions between an SR vesicle and the plasma membrane (Fig. 2A, between large arrows). Ordered arrays of feet (small arrows) occupy the junctional gap between the two membranes, zippering them together (Fig. 2A, E17, small arrows). Since feet have been identified as the cytoplasmic domains of RyRs, groups of feet in electron micrographs of peripheral couplings correspond to the foci of RyRs shown in Fig. 1.

Junctional plasma membrane domains are defined as areas of plasma membrane containing loose clusters of distinctive, large particles with an elongated shadow (outlined by arrowheads in Figs. 2B–2D, from freeze-fractures of myocardium at E10, E21, and adult). In previous work (Sun *et al.*, 1995), we established that the position of jPM corresponds to that of peripheral couplings seen in thin sections and that of DHPR clusters detected by immunohistochemistry. Also, the large particles were shown to constitute a unique population and to be similar to those identified as DHPRs in skeletal muscle. From these data, we suggested that the large particles represent DHPRs.

Development of Peripheral Couplings

The content of feet in peripheral couplings of developing myocardium is variable. In some ''incomplete'' junctions, feet are absent from the junctional gap (Figs. 3A, 3D, and 3G). In ''partially complete'' junctions, the feet are closely spaced in a portion of the gap, but are apparently absent elsewhere (Figs. 3B, 3E, and 3H). In ''complete'' junctions, the junctional gap is fully zippered by closely spaced feet (Figs. 3C, 3F, and 3I). At E2.5, we see incomplete junctions and a few partially complete ones, with two closely spaced feet in the junctional gap. At E4, such beginning groups of feet are more frequently and clearly seen (Fig. 3B), and we found one small complete junction. At E6, complete junctions are more frequent, although still of small size (Fig. 3C). The spacing between adjacent feet (arrows) is fairly

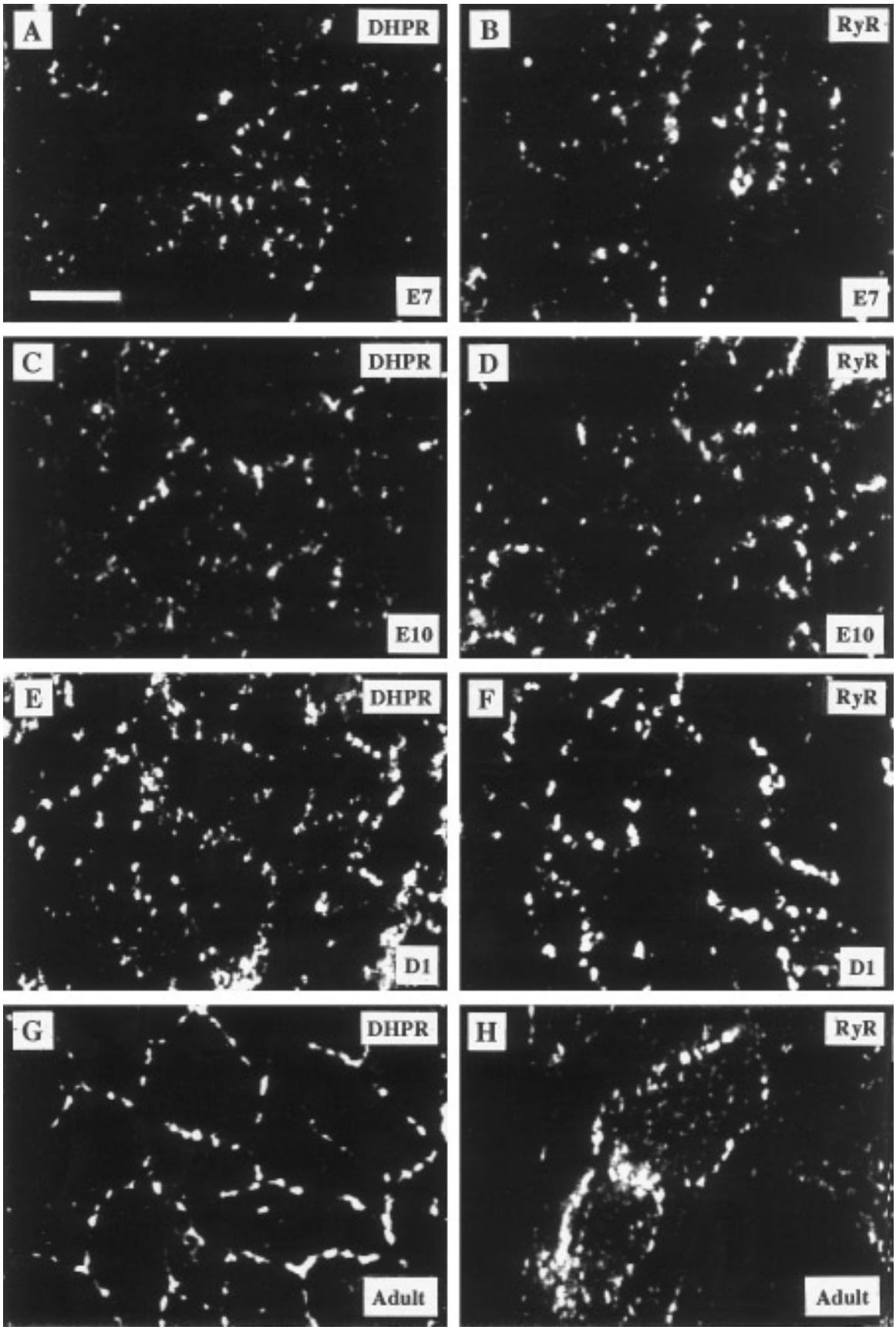
A
DHPR
E7
B
RyR
E7
C
DHPR
E10
D
RyR
E10
E
DHPR
D1
F
RyR
D1
G
DHPR
Adult
H
RyR
Adult

constant and thus we assume that the feet are part of an ordered array.

In areas of junctions where arrays of feet are missing, the gap is occupied by small, variably spaced densities. Occasionally, one of these densities appears to be a single foot (arrowhead in Fig. 3G), but identification is difficult in the absence of an array. In order to determine whether individual feet may be present in incomplete areas of junctions, we measured the width of the junctional gap. Thirty incomplete (from E2.5 to D6, 7 hearts), 7 partially complete (from E4 to adult, 4 hearts), and 64 complete junctions (from E4 to adult, 14 hearts) were selected (see Materials and Methods). In each junction, the gap was measured several times at different randomly chosen points, with some containing arrays of feet and others not. The average gap in regions clearly containing feet is 10.5 ± 0.1 nm (mean ± 1 SEM, from a total of 312 measurements) and in areas apparently without feet is 7.8 ± 0.2 nm (150 measurements). This difference is extremely significant (Student's t test, $P < 0.0001$). The gap in the incomplete areas of junctions is too narrow to accommodate feet, but about 11% of the measurements gave a gap of 10–13 nm, which is sufficient to accommodate a foot. This confirms the visual observation that feet are mostly missing from incomplete gaps, but individual feet may occasionally be present.

The width of junctional gap is not age dependent: the widths of feetless gaps at E2.5–E11 are slightly smaller than those at E13–adult, but the difference is marginally significant ($P < 0.076$), and the widths of feet-containing gaps at E4–E17 versus E18 to adult are not different from each other ($P < 0.438$).

Peripheral couplings also vary in the shape and luminal content of the SR vesicles forming them. Where feet are not visible, the SR vesicles have a variable shape and little content (Figs. 3A, 3D, 3G, 3E, and 3H, left side of the junction). On the other hand, where the junctional gap is zippered by arrays of feet, the SR has a characteristic flat shape and a dense content aligned to the junctional face of the vesicles (Figs. 3C, 3E, 3F, 3H, and 3I). This content, termed "junctional granules" (Sommer and Johnson, 1979; Sommer, 1995), presumably denotes an association of calsequestrin with the RyR-containing membrane. Formation of the junctional granules follows aggregation of feet: at E2.5 and E4, junctions have no dense content even when aggregates of 2–4 feet are seen (Fig. 3B), while at E6, most junctions with arrays of feet have a quite visible content, even when few feet are present (Fig. 3C and see also below).

Time Course of Peripheral Coupling Development

Changes with age in the relative frequencies of the various types of junctions are indicative of a gradual evolution. In Fig. 4A, the relative frequencies of incomplete (solid circles), partially complete (open circles), and complete (triangles) junctions are plotted against age. Incomplete junctions predominate at E2.5, become rapidly less frequent between E2.5 and E11, and are absent after E11. The relative frequency of partially complete junctions is low throughout, but it tends to decline gradually with age. Complete junctions are absent at E2.5–E4 (with one exception at E4); their frequency increases rapidly up to E11 and more gradually at later times.

Formation of the dense junctional granules in the lumen of the SR is slightly delayed relative to the aggregation of feet. Figure 4B plots the relative frequency of all junctions with two or more closely apposed feet (partially complete and complete junctions, solid circles) and that of junctions with a dense content associated with the feet (open circles). None of the junctions at E2.5–E4 have junctional granules, although some do have small arrays of feet. Between E2.5 and E4, all junctions with few feet have no granules; at E6 and E11 some of the junctions with arrays of feet have no granules; at E15 and later, all junctions with arrays of feet also have granules.

The results of Figs. 4A and 4B indicate a progressive transformation of incomplete junctions into complete ones, a hypothesis which is confirmed by the data below.

Incomplete Junctions: A Step in the Maturation of Peripheral Couplings?

Filling of the junctional gap by arrays of feet seems to be a gradual process, as indicated by the following data. Figure 5 shows the size of peripheral couplings measured from the profiles seen in thin sections. Two sets of data are plotted: triangles represent the total length of the junction, regardless of the presence or absence of feet; e.g., the length of membrane between arrows in Fig. 3A. Circles represent the length of the junction zippered by feet, i.e., either the zippered portions of partially complete junctions (left side of junction in Fig. 3B and right side of junctions in Figs. 3E and 3H) or the whole width of complete junctions (Figs. 3C, 3F, and 3I).

From these data, we obtain the following information. (i) The total length of the junctions remains approximately constant during development. The difference between averaged total length at E4–E14 (four hearts) versus that at D10 to adult (three hearts) is not significant ($P = 0.27$). (ii) The length of zippered junctions, on the other hand, increases with age. The difference between the averaged zippered length at E4–E14 (four hearts) versus that at D10 to adult (three hearts) is extremely significant ($P < 0.0001$). (iii) The zippered length is shorter than the total length of junctions

FIG. 1. Confocal images of cryosections from the left ventricle of chick myocardium, at ages E7 (A and B), E10 (C and D), D1 (E and F), and adult (G and H) immunolabelled for DHPRs (left) and RyRs (right). Discrete foci of the two proteins mark the profiles of single myocytes. Note the increase in size of myocytes between E7 and adult and the presence of RyR foci in the interior of the adult fiber. Bars, 10 μm.

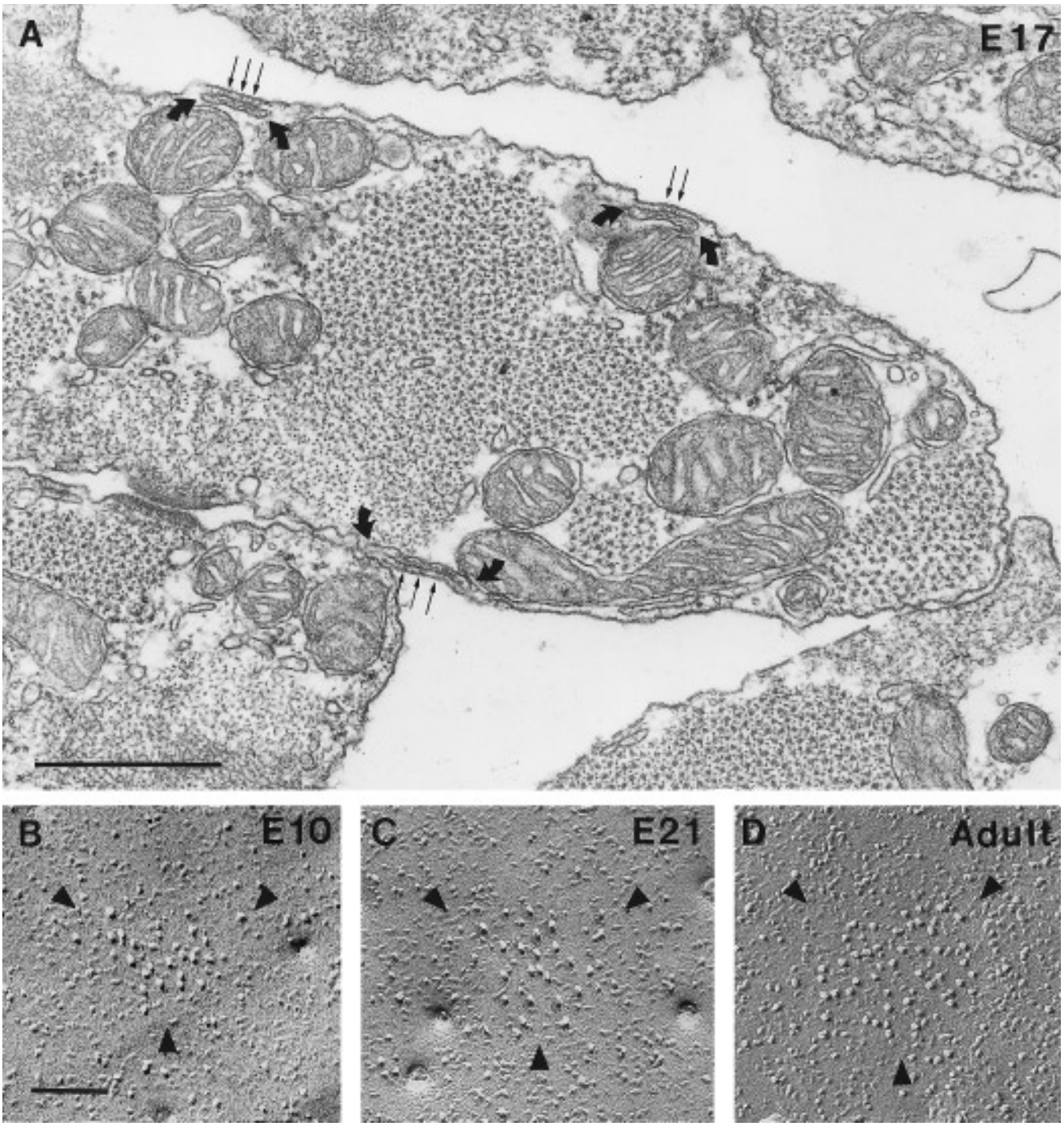

FIG. 2. (A) Cross section of cardiac myocytes at E17, showing peripheral couplings (between curved arrows) at the periphery of the muscle fibers. Feet (small arrows) occupy the junctional gap between sarcoplasmic reticulum cisternae and the plasma membrane. (B–D) Aggregates of large, tall intramembrane particles in junctional domains of the plasma membrane are outlined by arrowheads in these freeze-fracture images. The size of the domains increases with age (E10, E21, and adult are shown). Bars, (A) 0.5 μm; (B–D) 0.1 μm.

at early time points, but becomes similar at late time points. The difference between total and zippered lengths at E4–E17 (five hearts) is extremely significant ($P < 0.0001$). Student's t test of the difference between total and zippered lengths at D10 to adult (three hearts) indicates a marginally significant difference ($P = 0.1$), with the caution that this

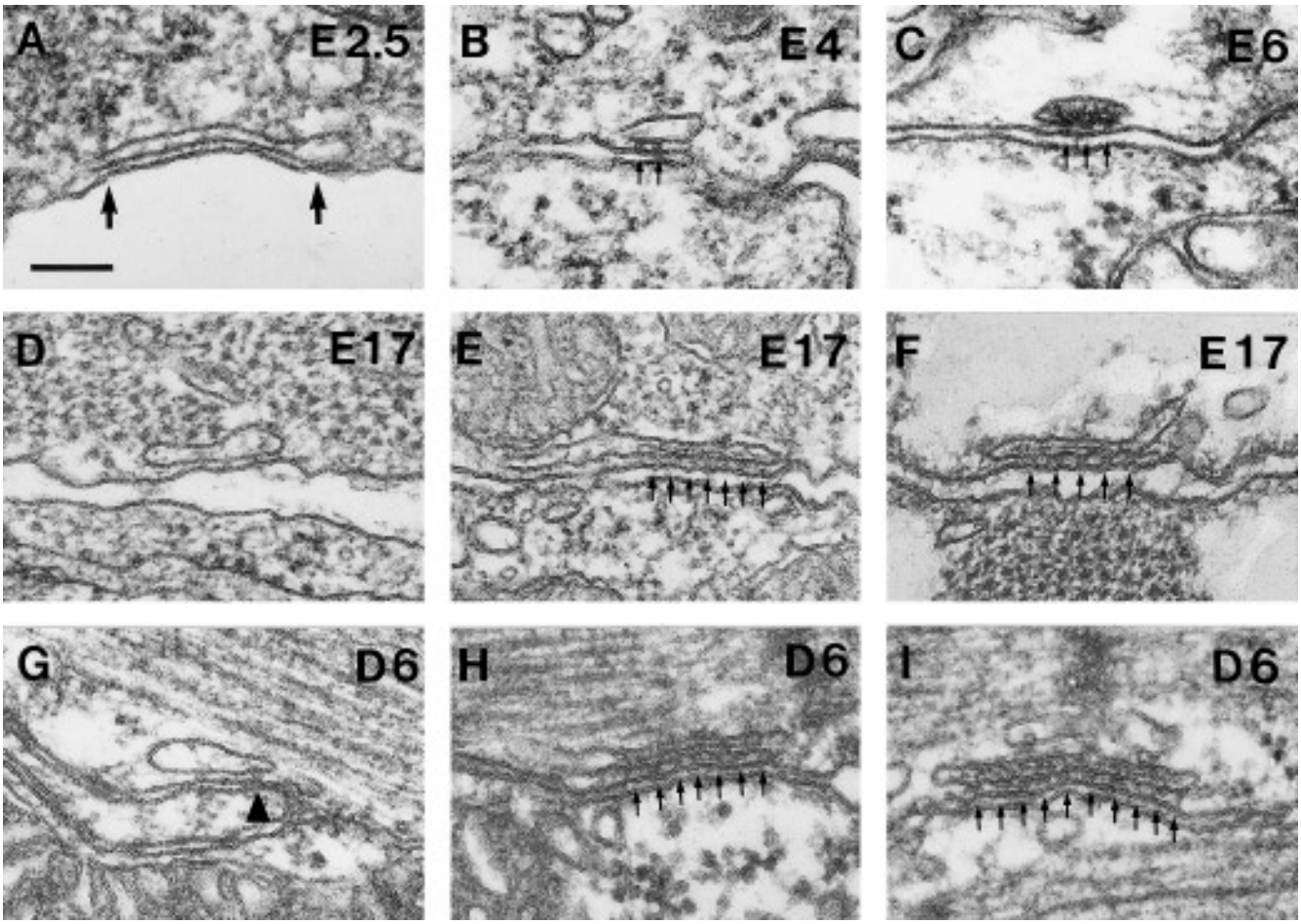

FIG. 3. Junctions between peripherally located cisternae of sarcoplasmic reticulum and the plasmalemma show various appearances. (A, D, and G) Incomplete junctions have either no feet (A and D) or, perhaps, a single foot (arrowhead in G) in the junctional gap. The size of the gap in these junctions is on the average smaller than the height of a foot. The content of the vesicles is ill defined. (B, E, and H) In partially complete junctions, evenly spaced feet (small arrows) are present in a portion of the junctional gap, but are missing elsewhere. The content of the SR vesicle (probably representing calsequestrin) forms a density associated with the feet-bearing portion of the junctional SR in E and H, but not in B. (C, F, and I) Complete junctions are totally zippered by arrays of evenly spaced feet and have a periodic dense content throughout. Bar, 0.1 μm.

is not precise, because the standard deviation is higher for one set of data (the triangles). Note that very few incomplete junctions ($<10\%$) are present at the late stages.

Parallel Development of Zippers and Particle Groups

The sizes of zippered junctions and plasma membrane junctional domains increase in parallel. Junctional domains of the plasma membrane containing large, tall particles are detected starting at E4 and become larger and more frequent with age (outlined by arrowheads in Figs. 2B–2D, 6A, 6D, and 6F). Groups of large particles are not detected at E2.5, possibly because the cells are very small, the membrane outlines very convoluted, and the junctional domains small and infrequent. Groups of two feet are detected at E2.5, but rarely. They were measured starting at E4 and their length also increases with age. The images in Fig. 6 give a visual impression of this development, showing increasing sizes of junctional domains (left) and arrays of feet (right) at E6, E17, and D6.

Figure 7A compares the measured surface areas of junctional domains (open circles) and the surface areas of feet arrays (solid circles), calculated from the data in Fig. 5 (see Materials and Methods). The two surface areas remain approximately equal to each other while more than doubling in size between E4 and adult. The difference in areas of junctional domains between E4 and E14 and D10 and adult (220 junctions, four hearts versus 193 junctions, three hearts) is extremely significant ($P < 0.0001$). The statistics for the diameters of feet arrays were done for the data in

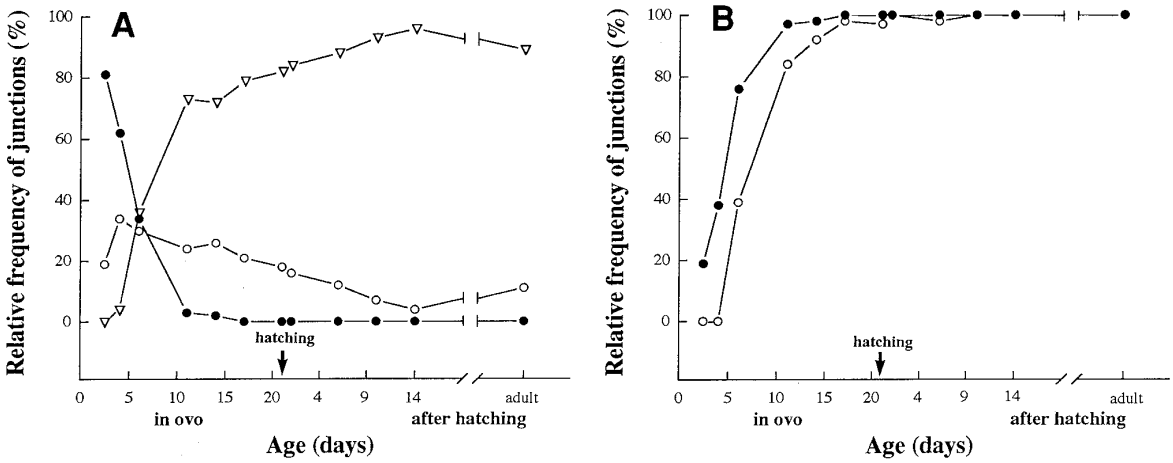

FIG. 4. (A) Changes in the relative frequency of incomplete (solid circles), partially complete (open circles), and complete (triangles) junctions with age. The frequency of incomplete junctions is very high at E2.5, and it declines to insignificant levels at E11. Partially complete junctions are more abundant in early than in later stages. Complete junctions are not present at E2.5 and E4, they are a minor component at E6, and they become predominant at E11 or later. The numbers are given as the percentage of total. Each time point on the graph is derived from a total of 38 to 184 junctions from one myocardium. (B) Comparison of the relative frequency of junctions with two or more closely spaced feet in the junctional gap (solid circles, partially complete and complete junctions) and of junctions that have a visible association of the SR vesicle content (presumably calsequestrin) with the feet-bearing SR membrane (open circles; see Figs. 3E, 3F, 3H, and 3I). At early time points, some vesicles have feet but lack a dense content. Sample size is the same as for A.

Fig. 5, and this also shows a significant difference between E4 and E14 (four heart) and D10 and adult ($P < 0.0001$). The two sets of areas cannot be compared statistically with each other, because the areas of feet arrays are extrapolated from their diameters (see legend to Fig. 7).

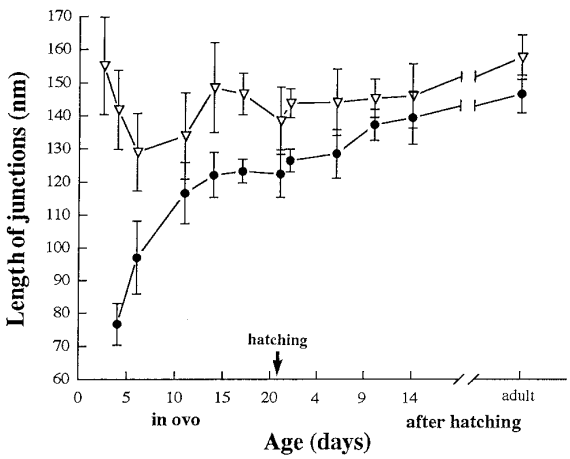

FIG. 5. Comparison between the total length of peripheral coupling profiles (triangles) and the length of profiles occupied by arrays of feet (circles). The "overall" length of junction remains approximately constant with age, but the length of junction "zippered" by feet increases with age. Triangles, 38–184 junctions from one myocardium at each time point (27 junctions at E2.5). Solid circles, 32–179 junctions from one myocardium at each time point (22 and 18 junctions for E4 and E6). Error bars, 1 SEM.

While the size of peripheral couplings increases with age, the spacing between feet and the density of particles in the junctional domains remain approximately constant (Fig. 7B). The particle density remains between 1086 and 1452 particles/μm^2, and the feet spacings are between 30.7 and 34.6 nm in myocardium from E4 to adult. Feet spacings and particle densities at E6–E14 are not significantly different from the spacings at D10 to adult. For feet spacings, $P = 0.14$, 69 junctions, five hearts versus 74 junctions, three hearts. For particle densities, $P = 0.2$, 220 junctions, four hearts versus 193 junctions, three hearts. Since the densities of the two proteins and the areas they occupy remain constant, their ratio also remains constant.

Maturation of the e–c Coupling Apparatus

As the heart develops, its fibers become more filled with contractile material, and the calcium handling capacity increases. One expression of this maturation process is the increase in frequency of peripheral couplings at the fiber periphery (Fig. 8): the number of junctions per unit length of plasma membrane increases by a factor of about 2.5 between E4 and E19 and then remains approximately constant. The difference in the frequency of peripheral couplings between E2.5 and E6 (300 counts and three hearts) and D19 and D3 (three hearts and 300 counts) is extremely significant ($P < 0.0001$), showing a large increase in the number of junctions.

A second maturation event is the development of internal feet-bearing SR, not associated with the plasma membrane (extended junctional SR, Jewett *et al.*, 1971). Extended junctional SR in chicken muscle first appears after hatching and

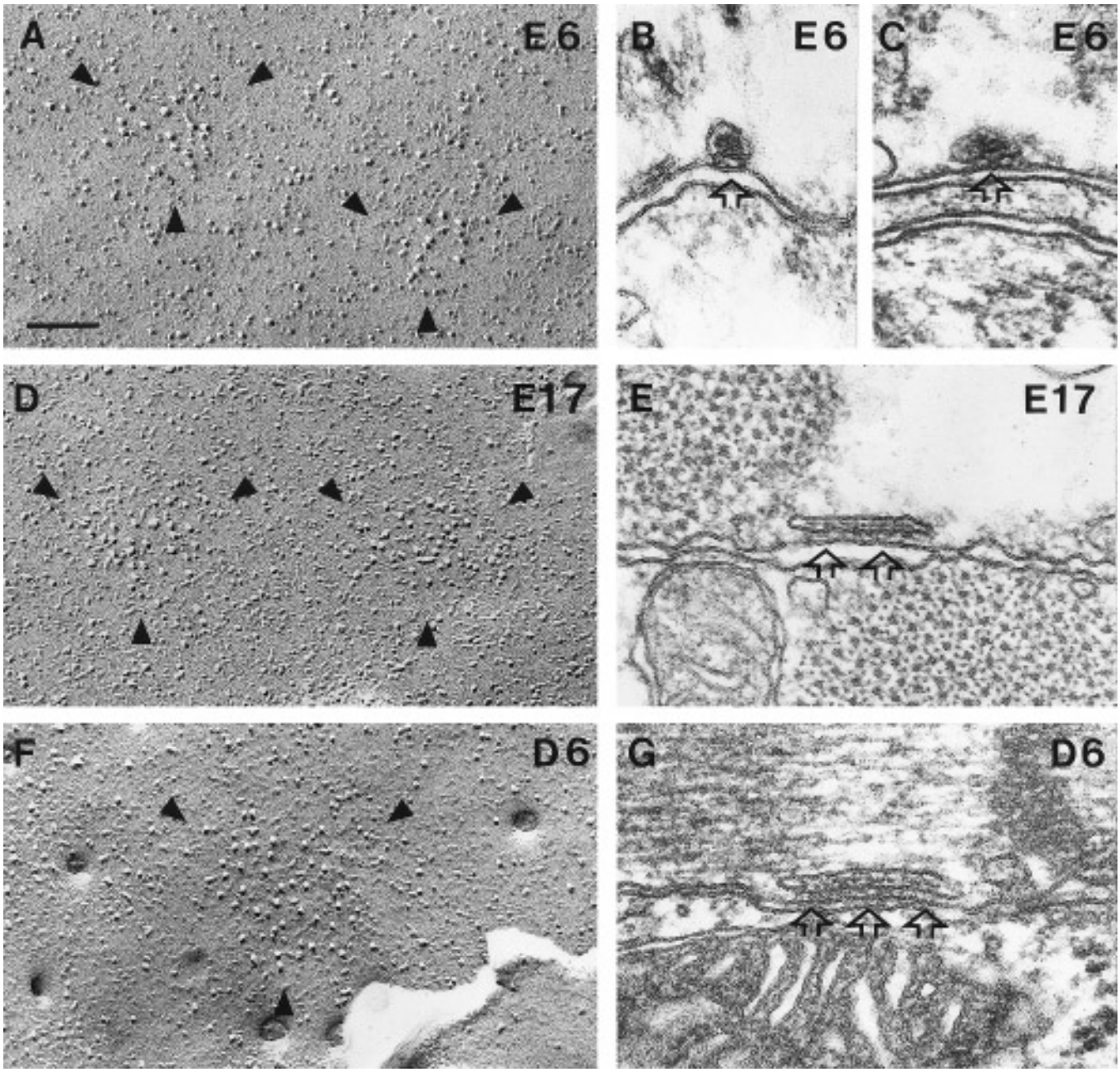

FIG. 6. Development of plasma membrane domains and peripheral couplings. (A, D, and F) The overall size of junctional domains increases with age, but the density of particles in them does not (E6, E17, and adult). (B, C, E and G) Arrays of feet within peripheral couplings also increase in size (B and C, E6; E, E17; G, D6). See also Figs. 7A and 7B. Bar, 0.1 μm.

increases in time (J. Sommer, personal communication; see also Fig. 1).

Finally, as in skeletal muscle, junctional SR is initially randomly disposed relative to the cross striation, but it gradually acquires a specific location, starting around hatching time. Figure 9B shows the surface of a cell at D14: the sarcomere spacing is clearly visible in the replica and the position of the Z line is marked by arrows. Each of the semicircles in Fig. 9B surround a plasma membrane domain of the type outlined by arrowheads in the enlargements (Figs. 9A and 9C). Most of these domains are located near the Z lines, although there are some clusters in different positions. Peripheral couplings (seen in thin sections) and clusters of DHPRs and RYRs (detected by immunohistochemistry) also show an increased tendency for a location in the proximity of the Z line during development (see Sun *et al.*, 1995, for more details).

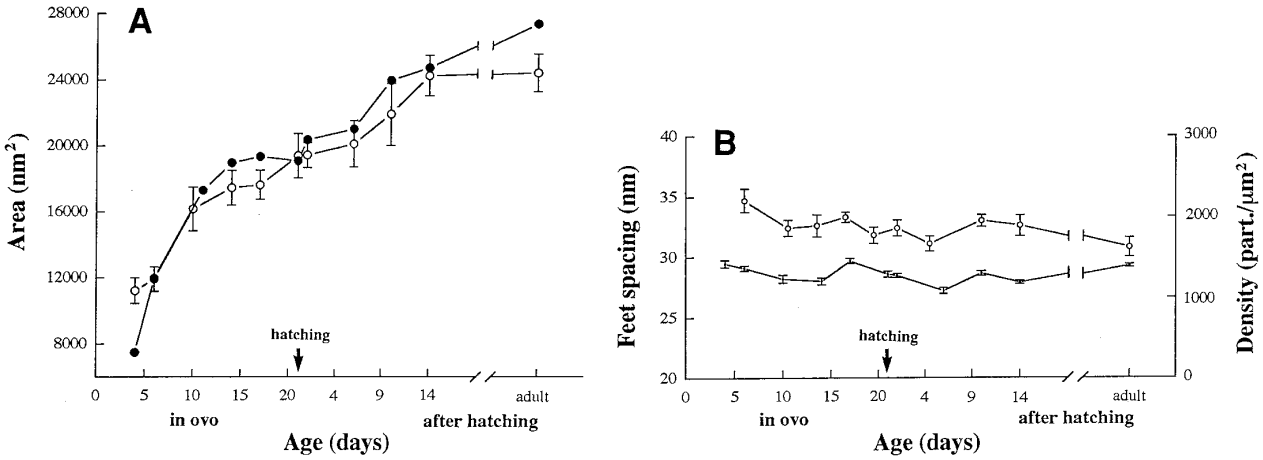

FIG. 7. (A) Comparison between areas of plasma membrane domains, measured from freeze-fracture replicas (open circles) and areas of arrays of feet (solid circles), calculated from data from Fig. 5. Averages for the two areas increase in size during development, but remain approximately equal to each other. The data for the feet arrays do not show a value for SEM, because sample variability includes the position of the section relative to the area, as well as the variability in the population of junctions. Sample size: open circles, 32–90 domains from one myocardium for each point; solid circles, 32–179 junctions from one myocardium (but 22 and 18 junctions at E4 and E6). Error bars, 1 SEM. (B) Spacing between feet (open circles, in nm) and density of junctional particles in plasma membrane domains (no symbol, number/μm^2) remain approximately constant throughout development. Thus, the densities of the two components of the junctions have a constant ratio. Sample size: 32–90 membrane domains and 14–63 feet arrays from one myocardium for each point. Error bars, 1 SEM.

DISCUSSION

The heart is a developmentally precocious organ: in the chick embryo, it starts to contract feebly and locally at about 30–33 hr of incubation, and it beats shortly after that (Romanoff, 1960). One important question is whether early myocardial activity relies on the same e–c coupling machinery that is used in the adult myocardium. RyRs have been detected in their ryanodine-binding tetrameric form as early as E4 (Dutro *et al.*, 1993). We find clusters of RyRs and DHPRs at E7 by using immunohistochemistry. Using electron microscopy, we also detect closely spaced feet (or RyRs) beginning at E2.5 and more clearly apparent at E4 and clusters of large plasma membrane particles (presumably DHPRs) at E4. We conclude that essential components of the e–c coupling machinery are not only present, but are also arranged within peripheral couplings (Carl *et al.*, 1995; Sun *et al.*, 1995) at a very early age, shortly after beating starts. However, we cannot be sure whether smaller, less easy to detect e–c coupling assemblies are present when local contractions are first seen.

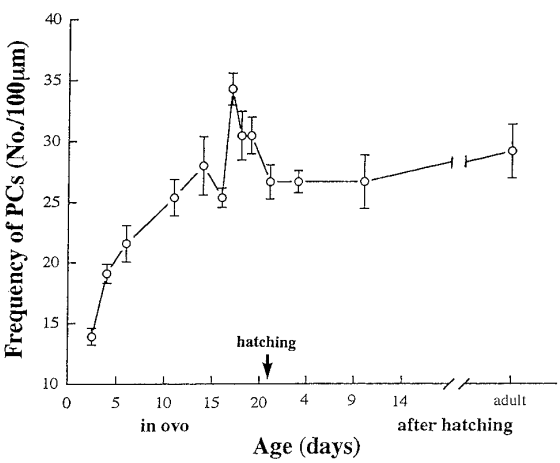

FIG. 8. Frequency of peripheral coupling profiles along the periphery of myocardial cells. The number of couplings per unit length (100 μm) of plasmalemma profile increases by a factor of about 2.5 between E4 and adult. Sample size: 100 counts (0.8-μm segments) and one heart for each time point. Error bars, 1 SEM.

The time course of formation of peripheral couplings gives clues to the development and function of the e–c coupling apparatus in cardiac muscle. Peripheral couplings form by a gradual accrual of feet within a narrow space (the junctional gap), which is formed by the docking of SR vesicles to the plasma membrane. This conclusion is based on three observations. (a) Entire junctions at early ages and portions of junctions at later ages have no visible feet and a gap which is too narrow to accommodate feet (see Radermacher *et al.*, 1994 for the foot height). (b) SR/surface junctions with few or no feet gradually decline in frequency, while junctions zippered by increasingly larger groups of feet become more numerous during development. The similarity in the average size of partially zippered and fully zippered junctions during early and late stages of development supports the gradual filling hypothesis. (c) The disposition of feet in partially complete junctions is uneven: feet are grouped on one side of the

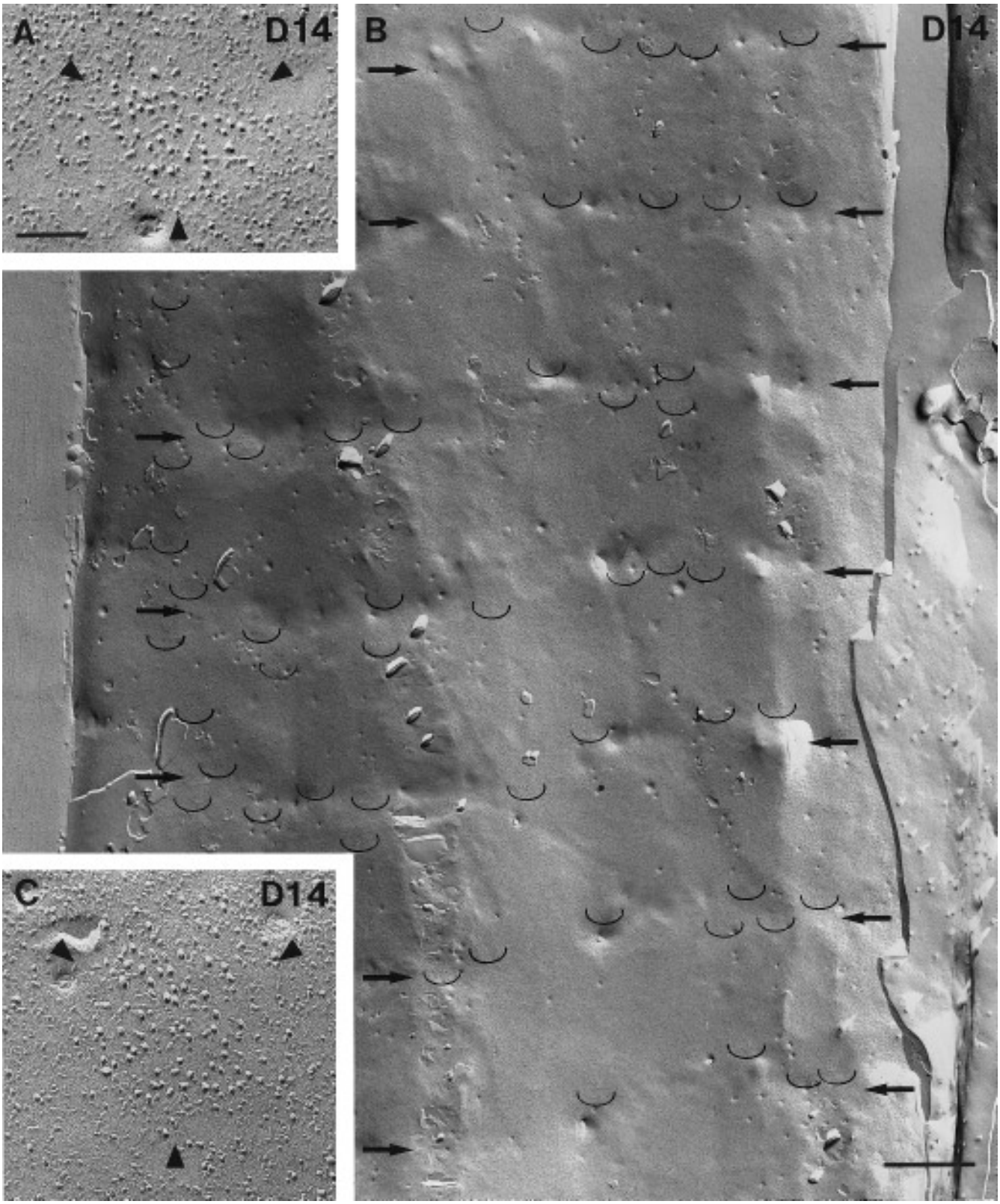

FIG. 9. (B) Relationship between cross striation and the position of surface domains in a myocardial cell at D14. Each semicircle surrounds a group of particles of the type shown, enlarged and outlined by arrowheads in A and C. Note a preferential location of these domains along and in proximity to the Z lines, whose position is indicated by arrows. Bars, (A and C) 0.1 μm; (B) 1 μm.

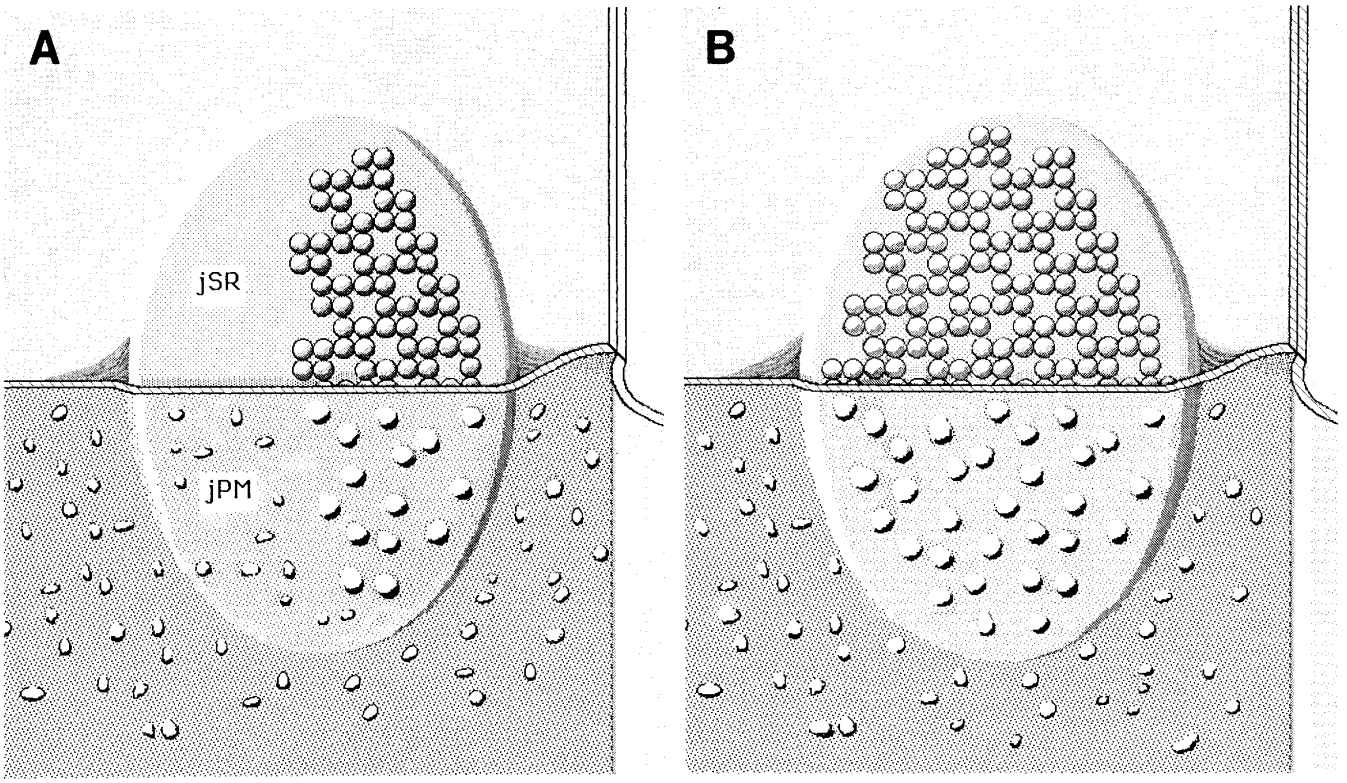

FIG. 10. (A) Reconstruction of a partially complete junction, extrapolated from our findings. The upper half of the image shows the junctional surface of an SR vesicle (jSR), which is partially covered by an array of feet. In the lower half, the image shows the split protoplasmic (inner) leaflet of the plasma membrane, facing the SR vesicle (jPM). Large membrane particles are restricted to the portion of jPM facing the array of feet. (B) Reconstruction of a complete junction. jSR and jPM are completely occupied by an array of feet and a cluster of large particles, respectively.

junction, leaving the other side empty. This is probably due to high affinity of the feet for each other, since feet form arrays in the absence of DHPRs and other muscle-specific junctional proteins, when RyRs are expressed in CHO cells (Takekura *et al.*, 1995b). Incomplete and partially complete junctions have also been observed in skeletal muscle and in a cell line of skeletal muscle origin (Edge, 1970; Marks *et al.*, 1991; Takekura *et al.*, 1995a).

Regarding the association of DHPRs with the junction, we note that jSR (containing feet) and jPM (containing large particles) grow in synchrony and that the ratio of feet to particles remains constant through development. Thus, accrual of the two major components of peripheral couplings is strictly coordinated. Figures 10A and 10B summarize our findings. In a developing junction (Fig. 10A), the array of feet and the group of large particles are limited to the same side of the junction. In the fully formed junction (Fig. 10B), feet and large particles completely occupy the facing junctional areas of SR and plasma membrane.

The close proximity of RyRs and DHPRs and the controlled ratio of the two proteins are early events in differentiation of cardiac muscle. We deduce that these two factors are crucial to the contractile function of early myocardium. The significance of the RyR–DHPR proximity has been discussed in terms of current hypothesis of cardiac e–c coupling (Sun *et al.*, 1995; Cannell *et al.*, 1995). We notice, however, that the large particles of junctional domains in cardiac muscle (presumably representing DHPRs) do not have a disposition indicating a link to the feet. This is in contrast to skeletal muscle (compare Sun *et al.*, 1995 with Block *et al.*, 1988; Franzini-Armstrong and Kisch, 1995). In view of the possible lack of direct interactions between particles and feet, the mechanism by which large particles are retained in the junctional domains of cardiac muscle remains a mystery.

We suggest that the formation of arrays of RyRs (feet) is the leading event in junction formation and that trapping of DHPRs (large particles) rapidly follows. This is supported by the following observations in the literature: feet form arrays independently of the presence of DHPRs in dysgenic skeletal muscle and in CHO cells (Franzini-Armstrong *et al.*, 1991; Takekura *et al.*, 1995b); grouping of DHPR fails in the absence of feet in dyspedic muscle (Takekura *et al.*, 1995a); and clusters of RyRs and DHPRs are colocalized through development and in adult skeletal and cardiac muscle (Jorgensen *et al.*, 1989; Flucher *et al.*, 1990; Yuan *et al.*, 1991; Carl *et al.*, 1995; Sun *et al.*, 1995).

The electron-dense content of the SR, due to the presence of calsequestrin (Jorgensen *et al.*, 1985), is associated with the feet-bearing areas of SR, indicating some interaction between feet and the protein responsible for linking calsequestrin to the junctional membrane. However, this association is detectable with a slight delay relative to the feet.

The relative frequencies of various types of junctions are indicative of the relative length of their lifespan. Our data suggest that during very early development (up to E6), filling of the gap by feet is slow relative to the rate of junction formation, perhaps due to low levels of RyR expression. After E6, filling of the gap with feet is rapid.

The maturation events in cardiac muscle membranes are an increase in the frequency of peripheral couplings, the after hatching appearance of the subsidiary internal calcium release system (extended junctional SR; Bossen *et al.*, 1978; Jorgensen *et al.*, 1993; Junker *et al.*, 1994; Sommer, 1995), and the redeployment of peripheral couplings from a random to a striation-related position. This latter event is quite similar to the striking rearrangement of transverse tubules and triads from a longitudinal to a transverse disposition in skeletal muscle (Franzini-Armstrong and Jorgensen, 1994; Takekura *et al.*, 1994b).

ACKNOWLEDGMENTS

We thank Drs. J. A. Airey, J. L. Sutko, M. Takahashi, and H. Takeshima for antibodies and Mrs. Nosta Glaser for excellent technical help. Supported by National Institute of Health Grant R01 HL48093.

REFERENCES

Airey, J. A., Beck, C. F., Murakami, K., Tanksley, S. J., Deerinck, T. J., Ellisman, and Sutko, J. L. (1990). Identification and localization of two triad junction foot protein isoforms in mature avian fast twitch skeletal muscle. *J. Biol. Chem.* **265,** 14187–14194.

Anderson, K., Lai, F. A., Liu, Q-Y., Rousseau, E., Erickson, H. P., and Meissner, G. (1989). Structural and functional characterization of the purified cardiac ryanodine receptor-Ca^{2+} release channel complex. *J. Biol. Chem.* **264,** 1329–1335.

Ashley, C. C., Mulligan, I. P., and Lea, T. J. (1991). Ca^{2+} and activation mechanisms in skeletal muscle. *Quart. Rev. Biophys.* **24,** 1–73.

Berridge, M. J., and Irvine, R. F. (1989). Inositol phosphates and cell signaling. *Nature (London)* **341,** 197–205.

Block, B. A., Imagawa, T., Campbell, K. P., and Franzini-Armstrong, C. (1988). Structural evidence for direct interaction between the molecular components of the transverse tubule/sarcoplasmic reticulum junction in skeletal muscle. *J. Cell Biol.* **107,** 2587–2600.

Bossen, E. H., Sommer, J. R., and Waugh, R. A. (1978). Comparative stereology of the mouse and finch left ventricle. *Tissue Cell* **10,** 773–779.

Cannell, M. B., Cheng, H., and Lederer, W. J. (1995). The control of calcium release in heart muscle. *Science* **268,** 1045–1049.

Carl, S. L., Felix, K., Caswell, A. H., Brandt, N. R., Ball, W. J., Vaghy, P. L., Meissner, G., and Ferguson, D. G. (1995). Immunolocalization of sarcolemmal dihydropyridine receptor and sarcoplasmic reticular triadin and ryanodine receptor in rabbit ventricle and atrium. *J. Cell Biol.* **129,** 673–682.

Catterall, W. A. (1991). Excitation–contraction coupling in vertebrate skeletal muscle: A tale of two calcium channels. *Cell* **64,** 871–874.

Dolber, P. C., and Sommer, J. R. (1984). Corbular sarcoplasmic reticulum of rabbit cardiac muscle. *J. Ultrastruct. Res.* **87,** 190–196.

Dutro, S. M., Airey, J. A., Beck, C. F., Sutko, J. L., and Trumble, W. R. (1993). Ryanodine receptor expression in embryonic avian cardiac muscle. *Dev. Biol.* **155,** 431–441.

Edge, M. B. (1970). Development of apposed sarcoplasmic reticulum at the T system and sarcolemma and the change in orientation of triads in rat skeletal muscle. *Dev. Biol.* **23,** 634–659.

Flucher, B. E., Morton, M. E., Froehner, S. C., and Daniels, M. P. (1990). Localization of the α_1 and α_2 subunits of the dihydropyridine receptor and ankyrin in skeletal muscle triads. *Neuron* **5,** 339–351.

Franzini-Armstrong, C., and Jorgensen, A. O. (1994). Structure and development of e–c coupling units in skeletal muscle. *Annu. Rev. Physiol.* **56,** 509–534.

Franzini-Armstrong, C., and Kisch, J. W. (1995). Alternate disposition of tetrads in peripheral couplings of skeletal muscle. *J. Muscle Res. Cell Motil.* **16,** 319–324.

Franzini-Armstrong, C., Pincon-Raymond, M., and Rieger, F. (1991). Muscle fibers from dysgenic mouse *in vivo* lack a surface component of peripheral couplings. *Dev. Biol.* **146,** 364–376.

Giannini, G., Conti, A., Mammarella, S., Scrobogna, M., and Sorrentino, V. (1995). The ryanodine receptor/calcium channel genes are widely and differentially expressed in murine brain and peripheral tissue. *J. Cell Biol.* **128,** 893–904.

Inui, M., Saito, A., and Fleischer, S. (1987a). Purification of the ryanodine receptor and identity with feet structures of junctional terminal cisternae of sarcoplasmic reticulum from fast skeletal muscle. *J. Biol. Chem.* **262,** 1740–1747.

Inui, M., Saito, A., and Fleischer, S. (1987b). Isolation of the ryanodine receptor from cardiac sarcoplasmic reticulum and identity with the feet structure. *J. Biol. Chem.* **262,** 15637–15642.

Jewett, P. H., Sommer, J. R., and Johnson, E. A. (1971). Cardiac muscle: Its ultrastructure in the finch and hummingbird with special reference to the sarcoplasmic reticulum. *J. Cell Biol.* **49,** 50–65.

Jewett, P. H., Leonard, S. D., and Sommer, J. R. (1973). Chicken cardiac muscle. *J. Cell Biol.* **56,** 595–600.

Jorgensen, A. O., Shen, A. C-Y., and Campbell, K. P. (1985). Ultrastructural localization of calsequestrin in adult rat atrial and ventricular cells. *J. Cell Biol.* **101,** 257–268.

Jorgensen, A. O., Shen, A. C-Y., Arnold, W., Leung, A. T., and Campbell, K. P. (1989). Subcellular distribution of the 1,4-Dihydropyridine receptor in rabbit skeletal muscle in situ: An immunofluorescence and immunocolloidal gold-labeling study. *J. Cell Biol.* **109,** 135–147.

Jorgensen, A. O., Shen, A. C-Y., Arnold, W., McPherson, P. S., and Campbell, K. P. (1993). The Ca^{2+} release channel/ryanodine receptor is localized in junctional and corbular sarcoplasmic reticulum in cardiac muscle. *J. Cell Biol.* **120,** 969–980.

Junker, J., Sommer, J. R., Sar, M., and Meissner, G. (1994). Extended junctional sarcoplasmic reticulum of avian cardiac muscle contains functional ryanodine receptors. *J. Biol. Chem.* **269,** 1627–1634.

Lai, F. A., Erickson, H. P., Rosseau, E., Liu, Q-Y., and Meissner, G. (1988). Purification and reconstitution of the calcium release channel from skeletal muscle. *Nature (London)* **331,** 315–319.

MacLennan, D. H., and Toyofuku, T. (1992). Structure–function relationships in sarcoplasmic or endoplasmic reticulum type Ca^{++} pumps. *Ann. N.Y. Acad. Sci.* **671,** 1–10.

Marks, A. R., Taubman, M. B., Saito, A., Dai, Y., and Fleisher, S. (1991). The ryanodine receptor/junctional channel complex is regulated by growth factors in a myogenic cell line. *J. Cell Biol.* **114,** 303–312.

Meissner, G. (1994). Ryanodine receptor/Ca^{2+} release channels and their regulation by endogenous effectors. *Annu. Rev. Physiol.* **56,** 485–508.

Pozzan, T., Rizzuto, R., Volpe, P., and Meldolesi, J. (1994). Molecular and cellular physiology of intracellular calcium stores. *Physiol. Rev.* **74,** 595–636.

Radermacher, M., Rao, V., Grassucci, R., Frank, J., Timerman, A. P., Fleisher, S., and Wagenknecht, T. (1994). Cryo-electron microscopy and three-dimensional reconstruction of the calcium release channel/ryanodine receptor from skeletal muscle. *J. Cell Biol.* **127,** 411–423.

Romanoff, A. L. (1960). ''The Avian Embryo. Structural and Functional Development.'' Macmillan, New York.

Sandow, A. (1965). Excitation-contraction coupling in skeletal muscle. *Pharmacol. Rev.* **17,** 265–320.

Sommer, J. R. (1995). Comparative Anatomy: In praise of a powerful approach to elucidate mechanisms translating cardiac excitation into purposeful contraction. *J. Mol. Cell Cardiol.* **27,** 19–35.

Sommer, J. R., and Johnson, E. A. (1979). Ultrastructure of cardiac muscle. *In* ''Handbook of Physiology''. (R. M. Berne, N. Sperelakis, and S. R. Geiger, Eds.), pp. 113–186. American Physiological Society, Bethesda, MD.

Stern, M. D., and Lakatta, E. G. (1992). Excitation–contraction coupling in the heart: The state of the question. *FASEB J.* **6,** 3092–3100.

Sun, X-H., Protasi, F., Takahashi, M., Takeshima, H., Ferguson, D. G., and Franzini-Armstrong, C. (1995). Molecular architecture of membranes involved in excitation-contraction coupling of cardiac muscle. *J. Cell Biol.* **129,** 659–671.

Takei, K., Mignery, G. A., Mugnaini, E., Sudhof, T. C., and De Camilli, P. (1994). Inositol 1,4,5-triphosphate receptor causes formation of ER cisternal stacks in transfected fibroblasts and in cerebellar Purkinkje cells. *Neuron* **12,** 327–342.

Takekura, H., Bennet, L., Tanabe, T., Beam, K. G., and Franzini-Armstrong, C. (1994a). Restoration of junctional tetrads in dysgenic myotubes by dihydropyridine receptor cDNA. *Biophys. J.* **67,** 793–804.

Takekura, H., Sun, X-Y., and Franzini-Armstrong, C. (1994b). Development of the excitation–contraction coupling apparatus in skeletal muscle. Peripheral and internal calcium release units are formed sequentially. *J. Muscle Res. Cell Motil.* **15,** 102–118.

Takekura, H., Nishi, M., Noda, T., Takeshima, H., and Franzini-Armstrong, C. (1995a). Abnormal junctions between plasma membrane and sarcoplasmic reticulum in skeletal muscle with a mutation targeted to the ryanodine receptor. *Proc. Natl. Acad. Sci. USA* **92,** 3381–3385.

Takekura, H., Takeshima, H., Nishimura, S., Takahashi, M., Tanabe, T., Flockerzi, V., Hoffman, F., and Franzini-Armstrong, C. (1995b). Co-expression in CHO cells of two muscle proteins involved in e–c coupling. *J. Muscle Res. Cell Motil.*, in press.

Yoshida, A., Takahashi, M., Nishimura, S., Takeshima, H., and Kokubun, S. (1992). Cyclic phosphorylation and regulation of the cardiac dihydropyridine-sensitive Ca^{2+} channel. *FEBS Lett.* **309,** 343–349.

Yuan, S., Arnold, W., and Jorgensen, A. O. (1991). Biogenesis of transverse tubules and triads: Immunolocalization of the 1,4-dihydropyridine receptor, TS28, and the ryanodine receptor in rabbit skeletal muscle developing in situ. *J. Cell Biol.* **112,** 289–301.

Received for publication July 17, 1995
Accepted October 10, 1995